Incoherent Neutron Scattering as a Probe of the Dynamics in Molecularly Thin Polymer Films

Christopher L. Soles,* Jack F. Douglas, and Wen-li Wu

NIST Polymers Division, Gaithersburg, Maryland 20899-8541

Robert M. Dimeo

NIST Center for Neutron Research, Gaithersburg, Maryland 20899-8562

Received June 17, 2002

ABSTRACT: Incoherent neutron scattering measurements were performed on polycarbonate (PC), poly(methyl methacrylate) (PMMA), and poly(vinyl chloride) (PVC) films of variable thickness, ranging from bulklike down to 75 Å, or length scales comparable to the polymer's radius of gyration. The temperature dependencies of the incoherent elastic scattering are analyzed in terms of a Debye−Waller factor to estimate the hydrogen-weighted mean-square atomic displacement $\langle u^2 \rangle$. We find a general reduction of $\langle u^2 \rangle$ as the polymer films become increasingly thin, especially above the calorimetric glass transition temperature, T_g. However, below T_g this reduction depends strongly upon the relative amplitude of the displacement. Specifically, if $\langle u^2 \rangle$ in the bulk glass is especially large, as seen in PC, the extensive sub-T_g motions are strongly suppressed by thin film confinement. On the contrary, glassy PVC displays comparatively small-amplitude displacements in the glass and virtually no reduction of $\langle u^2 \rangle$ upon confinement. These results are discussed in terms of a caging of the atomic motions as the degree of thin film confinement increases.

Introduction

Materials properties at surfaces and interfaces often deviate substantially from the bulk. For polymers, these deviations have potential ramifications in a range of thin film applications, such as photolithography, protective coatings, lubricants, and adhesives. Of particular interest are surface or thin film induced changes in the polymer mobility. Deviations in a polymer's dynamical properties could have deleterious effects on a variety of thin film applications. For example, an increase in the viscosity of an exceedingly thin hard disk lubricant film could lead to catastrophic failure of the drive. Conversely, increased molecular mobility in a very thin photoresist film could lead to enhanced photoacid diffusion and significant blur of the latent lithographic image. It is of both technical and scientific interest to understand how the molecular mobility of a polymer is affected by thin film confinement. In the following, we limit our discussion to polymer films that are supported on a rigid substrate.

A burgeoning body of literature addresses the issue of confinement and its effects on the mobility and glass transition of amorphous polymer thin films. To appreciate the wealth of research in this field, we refer to a recent review on glass transition phenomenon in thin polymer films.[1] Most experimental endeavors in this field focus on tracking the temperature dependence of some physical parameter, such as film thickness, index of refraction, etc. It is common to define a "kink" in the temperature dependence of this kind of data as the glass transition temperature, T_g, of the thin film and then to infer changes in the molecular mobility from shifts of this feature. A more direct approach is to probe changes in the local atomic or molecular mobility with neutron scattering. Neutrons are scattered from the nuclei and directly reflect the displacements at the atomic level. A large increase in the amplitude of these atomic motions occurs when a rigid amorphous solid softens into a viscous liquid, analogous to the melting of a crystal. Incoherent neutron scattering provides a useful means to monitor this motion and identify this dynamic transition.

In principle, inelastic neutron scattering spectra contain detailed information about the time scale and geometry of the atomic motions. Typically, the intensity of this inelastic scattering is several orders of magnitude smaller than the elastic scattering, especially in the glassy state. Unfortunately, this means that in a thin polymer film, where there is limited sample mass, the inelastic scattering is comparable to the experimental noise and exceedingly difficult to observe. However, the changes in the strong elastic scattering intensity also contain information, albeit less detailed, about the sample dynamics. This is because the total scattering must be conserved, and an increase in the inelastic scattering (i.e., an increase of mobility) necessitates a decrease in the elastic scattering. For elastic incoherent scattering, the Q dependence may be approximated by the Debye−Waller factor where

$$I_{\mathrm{inc,elastic}}(Q) \propto \exp\left(-\frac{1}{3}Q^2\langle u^2\rangle\right) \qquad (1)$$

Within this model, based on a harmonic solid, the slope in a plot of $\ln(I_{\mathrm{inc,elastic}}(Q))$ vs Q^2 is equal to $\langle u^2 \rangle/3$. While most atomic motions in soft condensed matter are admittedly anharmonic, this approximation has been useful characterizing the dynamics in both synthetic[2−6] and biological[7−11] macromolecules. Recently, we demonstrated that this approximation is also instructive for studying the confinement effect on the dynamics of thin polycarbonate films supported on Si substrates.[12] Here we build upon these initial measurements and examine three very different polymers to obtain a more complete understanding of how thin film confinement influences polymer dynamics.

10.1021/ma020952k
Published on Web 01/01/2003

Experimental Procedures

Thin films of polycarbonate (PC), poly(methyl methacrylate) (PMMA), or poly(vinyl chloride) (PVC) were spin-cast from solution onto clean Si wafers. The solutions were prepared by dissolving PC (GE Lexan ML-4235;[13] $M_{r,w}$ = 36.3 kg/mol), PMMA (Polymer Source; $M_{r,w}$ = 1730 kg/mol), and PVC (Aldrich; $M_{r,w}$ = 233 kg/mol) at various mass fractions into cyclohexanone, toluene, and cyclohexanone, respectively. These solutions were filtered through a 0.45 μm Teflon filter. Thin ⟨100⟩ Si wafers (Silicon, Inc.; 13−17 mils thick; 75 mm in diameter) were O_2 plasma cleaned to remove residual organic contaminants and treated with HF acid to remove the native silicon oxide surface. A controlled oxide layer was then regrown in a UV ozone chamber to a thickness of 10−20 Å. The polymer solutions were immediately spin-cast at 209 rad/s (2000 rpm) onto the clean, hydrophilic wafers to create the thin films. With some of the PMMA films, additional steps were taken to prepare a hydrophobic Si substrate. After the UV ozone exposure, hexamethlydisilizane was added dropwise onto the wafer and baked on a hot plate at 200 °C for 2 min. This replaces the surface Si−OH groups of the silicon oxide with $Si-CH_3$ groups, leaving a visibly hydrophobic surface. Immediately after spin-coating, the films were heated to $T_g + 20$ °C for at least 6 h under a vacuum better than 10^{-4} Pa to remove residual solvent. At this point, the film thickness was measured at room temperature with X-ray reflectivity.

The incoherent neutron scattering experiments were performed at the NIST Center for Neutron Research on the high-flux backscattering spectrometer[14] (HFBS), located on the NG2 beamline. This spectrometer utilizes cold neutrons with a wavelength of 6.271 Å and accesses a Q range of 0.25−1.75 $Å^{-1}$. This is important because the Bragg diffraction peaks for either the Si substrates or Al sample cell are beyond the Q range of the spectrometer and therefore not visible. The neutron absorption coefficients for both Si and Al are also low, ensuring that the hydrogenous polymer dominates the scattering. Likewise, the vibrational amplitudes in the crystalline Si are much smaller than any soft polymeric material, further ensuring that the dynamics of the Si are negligible. The 0.8 μeV full width half-maximum energy resolution of the spectrometer dictates that only those motions 200 MHz or faster will contribute to the decrease in the elastic scattering; slower motions appear as elastic scattering.

The HFBS sample cells were thin-walled Al cans approximately 25 mm in diameter and 50 mm high. To maximize the scattering signal from our thin polymer films, we cleaved 13−15 of the coated wafers into 50 mm strips (of varying width) and placed them in the sample cell. This resulted in approximately 0.5−10 mg of the polymer per cell vs 52−58 g of Si. The sample cell was then mounted on the HFBS spectrometer, placed under a vacuum, and cooled to 30−50 K. Data were collected as the samples were heated at a rate of 0.1−0.5 K/min up to 525 K. The scattered intensities in each detector (each Q; there are 16 detectors) were summed over temperature intervals of 1−3 K to increase the counting statistic. Slower heating rates were required for the thinner films in order to obtain reasonable counting statistics. The measurement times for the thinnest films are on the order of 3−4 days.

Results and Discussion

Data Interpretation. Figure 1 displays the temperature dependence of the elastic scattering intensity, summed over the entire Q range of the spectrometer, for the oxide-supported PC, PMMA, and PVC films. The intensities are normalized to one at their lowest temperature so as to compare the films of different thickness. As mentioned above, an intensity decrease corresponds to an increase in the amplitude of the atomic motion, which we interpret as an increase in mobility. As Figure 1 demonstrates, the HFBS spectrometer has sufficient sensitivity to probe the dynamics in films as thin as 75 Å. This figure also indicates that extent of mobility is reduced as the film thickness decreases. The thermal reduction of the elastic intensity becomes less significant in the increasingly thin films. By analyzing the Q dependence of these changes, one can estimate the mean-square atomic displacements $\langle u^2 \rangle$ from eq 1.

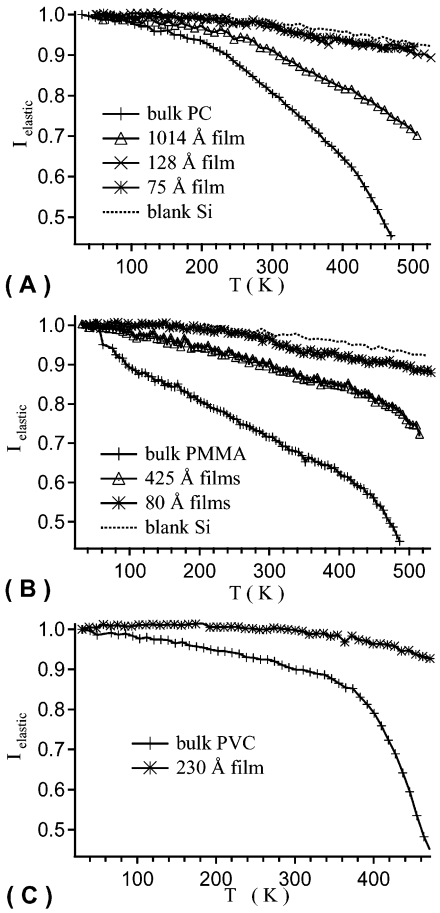

Figure 1. Elastic neutron scattering intensity, summed over all available detectors, is displayed as a function of temperature for the PC, PMMA, and PVC films. For each sample, the intensities are normalized by their lowest temperature value. The decrease in intensity upon heating directly reflects the thermal motion in the polymer film. As film thickness decreases, there is a strong reduction of this thermal mobility. The standard uncertainties in the scattered intensities are less than or comparable to the size of the data markers.

The Q dependence of the elastic scattering as a function of temperature for the thinnest PC and PMMA films is shown in Figure 2. Again, the lowest temperature, which is generally between 30 and 50 K, normalizes the elastic intensity. According to the Debye−Waller approximation, a normalized $\ln(I_{elastic})$ vs Q^2 plot yields a straight line with the slope proportional to $\langle u^2 \rangle / 3$. For the 75 Å PC film, we see that the linear approximation is reasonable for the Q^2 range below 1.0 $Å^{-2}$. However, the inset reveals deviations from linearity above $Q^2 = 1.0$ $Å^{-2}$, with an apparent maximum near $Q^2 = 1.5^{-2}$ $Å^{-2}$ in both the bulk and thin film data. Previously, we noted that this maximum nominally coincides with the peak in the static structure factor, commonly referred to as the amorphous halo ($Q^2 = 1.6$ $Å^{-2}$).[12] From this we surmised that the strong deviation from linearity in PC indicates coherent neutron scattering, especially at high temperatures where the deviation is most pronounced.

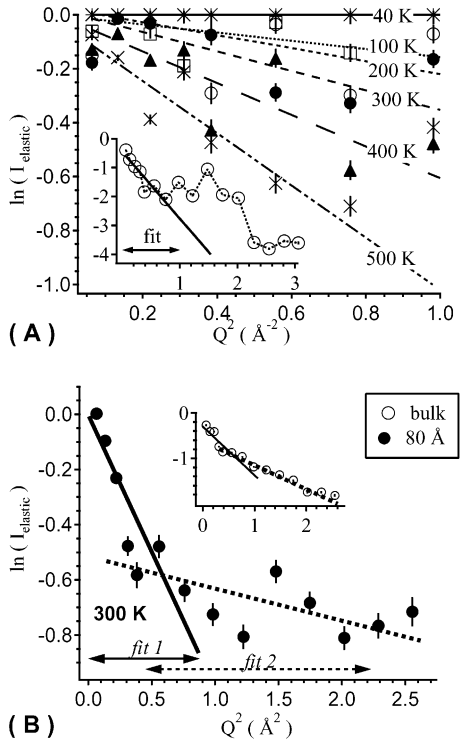

Figure 2. Graph demonstrating the typical $\ln(I_{elastic})$ vs Q^2 plots needed to estimate $\langle u^2 \rangle$. In this representation, $\langle u^2 \rangle$ is proportional to the slope of a linear fit through the data. In (A), the main portion of the graph shows isothermal fits for the 75 Å PC film from the region $Q^2 < 1.0$ Å^{-2}. As temperature increases, the larger slope corresponds an increase of $\langle u^2 \rangle$. The inset of (A) displays an analogous plot for the bulk PC at 300 K. Notice that the peak in the bulk data near $Q^2 = 1.5$ Å^{-2}. Possible origins of this peak, which is also present in the thin film data, are discussed in the text. Likewise, (B) shows the same type of data for the bulk and 80 Å PMMA films. In PMMA, the bulk data reveal two quasi-linear regimes. The implications of using the two different fitting regimes are discussed later. Error bars indicate the standard uncertainty in the scattered intensity.

In addition to PC, Figure 2 shows the $\ln(I_{inc})$ vs Q^2 curves for PMMA at 300 K in the both the 80 Å films and the bulk (inset). As with the PC, the region below $Q^2 = 1.0$ Å^{-2} is reasonably linear in both the thin film and bulk. In the region beyond $Q^2 = 1.0$ Å^{-2}, the PMMA dependence is now linear, without the maximum that is evident in the PC. Although it is not explicitly shown here, the Q dependence of the PVC elastic intensities qualitatively resemble PMMA. At this time we do not completely understand why PC differs from PMMA and PVC in the high-Q region. Regardless of their differences at high Q, the PC, PMMA, and PVC show similar trends in the low-Q region, and there is always a break in the slope near $Q^2 = 1.0$ Å^{-2}. This reflects that fact the motions are considerably more complicated than predicted by the harmonic Debye−Waller model. Nonlinear dependencies of $\ln(I_{inc})$ on Q^2 have been reported in a number of polymer[3] and biological[7,9,10,15] systems, and there have been attempts to calculate $\langle u^2 \rangle$ using more complicated models. These models generally embody both a Gaussian (harmonic) and a non-Gaussian component, with the latter being thermally activated and dominant at low Q.[3,7,9,10,15] However, these models also increase the number of curve fitting parameters so it is not entirely clear whether the added parameters truly increase our understanding of the motions. Furthermore, one must fit the data to very high Q to reliably separate the local harmonic motions (high Q) from the long-range anharmonic contributions (low Q). The HFBS spectrometer is not designed to access these high-Q regions of phase space.

Given the Q range of our spectrometer and the thin film data presented above, we take a simplified approach and limit the $\langle u^2 \rangle$ analysis, using the simple harmonic model in eq 1, to the regime below $Q^2 = 1.0$ Å^{-2}. This region appears to be consistent between different types of polymers and avoids peaklike features or upturns in the high-Q data. Of course, the $\langle u^2 \rangle$ values extracted from this harmonic approximation are not exact in light of the anharmonicity evidenced in Figure 2. In this respect it has been demonstrated that analyzing this low-Q data overemphasizes some of the long-range anharmonic motions, such as methyl rotations.[3] Nevertheless, the low-Q estimate of $\langle u^2 \rangle$ provides a reasonable and consistent framework to compare thin film confinement effects between the different polymers. We demonstrate the generality of this approach with the PMMA films, where absence of the strong high-Q peak in PMMA allows one to fit two linear functions (one low and one high Q) through the data, as seen in Figure 2. This allows us to compare the $\langle u^2 \rangle$ trends from the low- and high-Q regions. As will be demonstrated below, while the absolute values of $\langle u^2 \rangle$ determined from two regions differ, the trends with confinement are similar.

The differences between the low- and high-Q estimates of $\langle u^2 \rangle$ are evident in Figure 3. Choosing to analyze the lower Q region (Figures 3A−C) leads to slightly larger $\langle u^2 \rangle$ values. At 395 K, the calorimetric T_g of PMMA, $\langle u^2 \rangle$ is nearly 1.3 Å^2 when the analysis focuses on the region $Q^2 < 1.0$ Å^{-2}, while $\langle u^2 \rangle$ is 0.8 Å^2 for the region $0.5 < Q$ (Å^{-2}) < 2.5. This is reasonable since the low-Q data reflect longer-range motions. What is more important is to appreciate that the trends with decreasing film thickness are similar for the two regions. Both show a general reduction of $\langle u^2 \rangle$ with decreasing film thickness and insignificant differences between the passivated (HMDS) and oxide surfaces. So while focusing on the low-Q region may emphasize longer-range motions that potentially deviate from the harmonic Debye−Waller criteria at high temperature, the general indication of how the dynamics respond to confinement are reasonable. This should be borne in mind when considering the absolute magnitudes of $\langle u^2 \rangle$ in this work. For consistency, all of the $\langle u^2 \rangle$ values reported here come from the region $Q^2 < 1.0$ Å^{-2}.

Likewise, Figure 3 displays the low-Q estimates of $\langle u^2 \rangle$ as a function film thickness and temperature for the PC and PVC films. Once again, the general trend is that decreasing film thickness leads to a suppression of $\langle u^2 \rangle$. However, in PVC this suppression is primarily observed above the bulk calorimetric T_g of 358 K; deep in the glassy state there is very little change in $\langle u^2 \rangle$ with increasing confinement. This is unlike the PC films (and to a lesser extent the PMMA films), which exhibit large suppressions of $\langle u^2 \rangle$ far below the bulk calorimetric T_g.

$\langle u^2 \rangle$ and Effects of Thin Film Confinement on Polymer Dynamics. A comparison of the thin film confinement effects in different polymers should account for natural differences in the characteristic dimensions of the macromolecules. For example, a high molecular mass polymer would feel the conformational effects of confinement in thicker films than its low molecular mass analogue. In this respect it is reasonable to

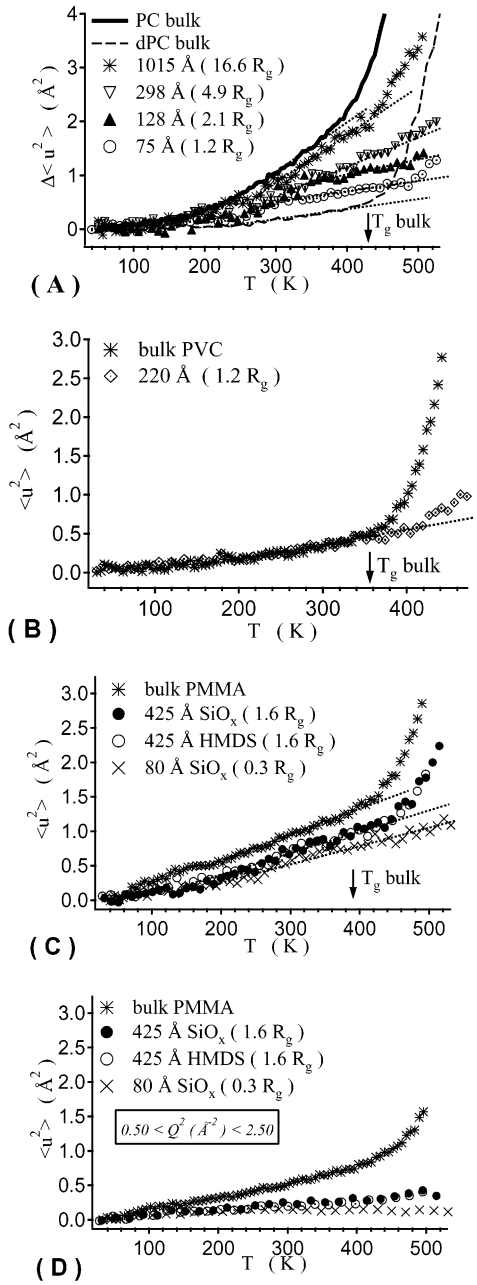

Figure 3. Hydrogen-weighted mean-square atomic displacements $\langle u^2 \rangle$ plotted as a function of temperature for the PC, PMMA, and PVC films. These data are obtained from linear fits from the region $Q^2 < 1.0$ Å^{-2} as demonstrated in Figure 2. The legend within each plots indicates the film thickness in terms of the units of the unperturbed chain dimensions, i.e., R_g. There is also an alternative data set for PMMA that demonstrates the differences in $\langle u^2 \rangle$ that originate from using the different linear fitting regimes denoted in Figure 2. While the magnitudes of $\langle u^2 \rangle$ are strongly affected by the choice of the fitting regime, the trends as a function of film thickness are qualitatively similar. With regards to PC, the dPC curve demonstrates how $\langle u^2 \rangle$ can be significantly altered by replacing all of the hydrogen in PC with deuterium. The standard uncertainties in $\langle u^2 \rangle$ are typically comparable to the size of the data markers.

normalize the film thickness h in terms of the molecular size or the radius of gyration R_g. R_g estimates for the PC, PMMA, and PVC under Θ conditions are 61,[16] 262,[17] and 179 Å,[18] respectively. The legend in Figure 3 correspondingly indicates the film thickness in multiples of the ideal chain R_g. This normalization suggests that the polymers in the thinnest films are highly confined, with an overall thickness less than the unperturbed diameter (approximately one R_g) of the macromolecule.

Figure 3 suggests a correlation between the magnitude of $\langle u^2 \rangle$ in the bulk and the degree to which there is a suppression of $\langle u^2 \rangle$ below the calorimetric glass transition. For example, PC has both the largest mean-square displacements and the strongest suppression of $\langle u^2 \rangle$. At the calorimetric T_g (425 K), the bulk $\langle u^2 \rangle$ is 2.4 Å^2 in PC but diminished to 0.7 Å^2 in the R_g-thick film. This corresponds to a reduction of 71%. For PMMA the bulk $\langle u^2 \rangle$ at the calorimetric T_g (395 K) is smaller, 1.3 Å^2, with a decrease to 0.7 Å^2 in the R_g-thick film. This 46% reduction of $\langle u^2 \rangle$ is less dramatic in PMMA in comparison to PC. In contrast, the $\langle u^2 \rangle$ is exceedingly small in bulk PVC at T_g (358 K), on the order of 0.5 Å^2. Correspondingly, there is no reduction of $\langle u^2 \rangle$ in the R_g-thick PVC film.

The sizable $\langle u^2 \rangle$ values in bulk PC are reasonable. PC is well-known for its extensive segmental or local molecular mobility in the glassy state. This in part reflects why PC has such a superb toughness or impact resistance; extensive molecular mobility provides pathways to rapidly dissipate strain energy. The types of motions that occur (in concert) deep within the glassy state include librations/rotations of the isopropylidene methyls,[19−23] π-flips of the phenyl rings,[21,24−27] and cis−trans isomerizations of the carbonate moieties.[19,28−31] The first two of these groups are hydrogenous and therefore dominate $\langle u^2 \rangle$ because of their large incoherent scattering cross section. To appreciate how much the localized methyl and phenyl ring motions dominate $\langle u^2 \rangle$, it is instructive to study deuterium-substituted PC. Replacing the hydrogen with deuterium atoms greatly reduces the incoherent scattering cross section, making the scattering mostly coherent. In terms of coherent scattering, the contributions from C, D, and O are comparable, and the motions specific to the methyl groups or phenol rings are thereby deemphasized. The $\langle u^2 \rangle$ values for the corresponding deuterated PC (bulk) in Figure 3 are significantly less than the hydrogenated analogues, especially below T_g. It is worth mentioning that the Q dependences of the hydrogenated and deuterated samples are quite similar. Thus, we do not believe that coherency effects substantially distort the $\langle u^2 \rangle$ values extracted from the data (recall earlier discussions where the hydrogenated PC appeared to have a noticeable coherent scattering). In the deuterated PC $\langle u^2 \rangle$ evolves linearly (harmonically) with T and attains a value of just 0.5 Å^2 at the calorimetric glass transition. This is in stark contrast to the hydrogenated PC, where $\langle u^2 \rangle$ is 2.4 Å^2 at the same T.

The implications here are clear. The large $\langle u^2 \rangle$ in glassy PC films reflect segmental or localized motions, not long-range motions of the main chain. Such diffusive motions, which give rise to viscous flow, do not occur until the T_g is exceeded. This is clear from the deuterated PC where $\langle u^2 \rangle$ becomes appreciable only above T_g. This is analogous to the bulk (and thin film) PVC where $\langle u^2 \rangle$ does not increase significantly until one enters the rubbery state. However, the hydrogenous species are not masked in the case of PVC; rather, they are directly connected to main chain in a comparatively immobile fashion (the hydrogen motion directly reflects the motions of the chain). Returning to the analogy with mechanical properties, this is also consistent with the picture of PVC as brittle glass with very few molecular mechanisms to dissipate strain energy. In fact, it is well-

known that PVC needs plasticizers or diluents to enhance the molecular mobility and promote ductility at room temperature.[32]

These observations are intriguing because they point to the notion that highly dynamic glasses, with extensive segmental mobility below the calorimetric T_g, are more susceptible to confinement below the glass transition. That $\langle u^2 \rangle$ is severely curtailed in the thin PC films then raises the question whether the mechanical and physical properties of PC change in the highly confined thin films. Other studies have shown that freezing these motions via synthetic routes, i.e., imposing steric restrictions, transforms the normally ductile and tough PC into a brittle plastic.[33,34] It is therefore plausible that a similar effect is induced by the state of confinement in the thin films. It is observed that onset of these phenyl ring flips and methyl rotations in bulk PC coincides[35,36] with the sub-T_g relaxation (we do not imply that these motions are necessarily the origin of this relaxation) near 175 K that is commonly referred to as the β- or γ-relaxation in dielectric or dynamic mechanical spectroscopy. The severe reduction of $\langle u^2 \rangle$ in the thin PC films might then point to a suppression of this characteristic sub-T_g relaxation and therefore potentially a fundamental change in the nature of the glassy state.

On some levels it is remarkable that the highly localized motions reflected in $\langle u^2 \rangle$ can be affected when the film thickness is orders of magnitude greater than the amplitude of the motion. For example, intuition tells us macromolecular dimensions typically do not affect local or segmental motions, such as sub-T_g relaxations. However, if thin film confinement alters the conformation that in turn affects the nature of the intra- and intermolecular packing, one might also anticipate changes in the highly local motions. A reduction of $\langle u^2 \rangle$ could then be rationalized if molecules are packed tighter, more strongly caged by their neighboring segments.

$\langle u^2 \rangle$ and the Glass Transition in Thin Polymer Films. Up to this point, we have not discussed how $\langle u^2 \rangle$ relates to the glass transition temperature in thin polymer films. In a wide variety of glass forming liquids, it is well documented that $\langle u^2 \rangle$ goes through a sharp increase at the calorimetrically defined glass transition temperature,[2,4,6,8,37,38] consistent with the sudden drop in viscosity. Extending this phenomenology to thin films, Figure 3 would seem to indicate that confinement leads to a T_g *increase* for all of these polymers. This conclusion, however, is not so clear when we consider complementary data. For example, X-ray reflectivity measurements of the PC film's thermal expansion indicate an *opposite* trend, a T_g decrease in the 75 Å film.[12] To further clarify this situation, we compare X-ray reflectivity, beam positron annihilation lifetime spectroscopy (PALS), and incoherent neutron scattering measurements on an identical set of PC films.[39] While the details of this study are not described here, both X-ray reflectivity and PALS suggest a decrease in the apparent T_g while neutron scattering points to an increase. Likewise, optical[40,41] and thermal probe studies[42] of PMMA films on SiO_x and HMDS substrates appear to indicate an opposite conclusion regarding a T_g shift in comparison to our neutron scattering. These techniques predict a T_g increase for the R_g-thick film on the SiO_x substrate and a T_g decrease on the HMDS surface. Clearly, their HMDS substrate data are in contrast to our $\langle u^2 \rangle$ data in Figure 3, which does not immediately support a reduced T_g. Unfortunately, the origin of this discrepancy between the neutron scattering and other techniques for estimating T_g in thin polymer films is unclear. The fact that the different techniques are exacerbated differently by confinement is, however, intriguing.

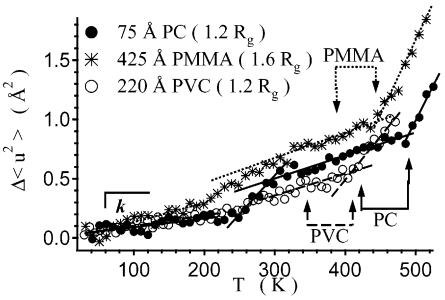

Figure 4. Comparison of PC, PMMA, and PVC films that are all approximately one R_g thick. The expanded vertical scale (in comparison to Figure 3) reveals greater detail in the thermal evolution of $\langle u^2 \rangle$. For each curve, there are two sets of vertical arrows. In each instance the left arrow indicates the calorimetric T_g determined from the bulk material while the right arrow corresponds to $1.2T_g$ and a strong increase of $\langle u^2 \rangle$. The implications of this are discussed in the text. This plot also demonstrates the low-temperature linear regime, below 200 K, where κ the vibrational spring constant is determined (see Figure 5 and the discussion). Vertical error bars denote the standard uncertainty in $\langle u^2 \rangle$.

It is worth emphasizing that T_g shifts are normally inferred from changes in a thermodynamic property measurements (specific heat, thermal expansion, etc.) performed under *nonequilibrium* conditions. A frequency or time scale is always implicit in these measurements, dependent upon the rate at which the property is probed. It seems likely the time scales over which a polymer equilibrates could be quite different in thin films as compared to the bulk and that these changes could be *property specific* (dependent on the frequency scale of the measurement). It is well-known from surface forces apparatus measurement on confined liquid films (both polymer and small molecule) that the viscoelastic time scales in the bulk and molecularly confined films are generally not the same.[43−46] In this respect it is unclear whether the thin film measurements are comparable to the bulk. Therefore, we must be careful when relating the kink in various thermodynamic properties as a function of temperature to the glass transition; the relation may not be straightforward.

It is interesting to examine the thermophysical behavior in the thinnest of the PC, PMMA, and PVC films. Figure 4 compares mean-square displacement in all three of the polymers when they are confined to an R_g-thick film. In contrast to Figure 3, the expanded vertical scale reveals greater detail in the thermal evolution $\langle u^2 \rangle$. For each polymer, a set of two connected vertical arrows are superimposed on the graph. In each case, the left-most arrow, which does not coincide with a distinct feature on the curve, corresponds to the bulk calorimetric T_g. The right-most arrow, which coincides with the strong upturn in $\langle u^2 \rangle$, indicates a temperature equal to $1.2T_g$. This coincidence is striking and provocative. In fragile glass-forming liquids, a number of distinct changes are known to occur at an upper transitional temperature commonly near $1.2T_g$ (in the so-called strong glasses this transition is closer to $1.5T_g$). These changes include, but are not limited to, deviations from

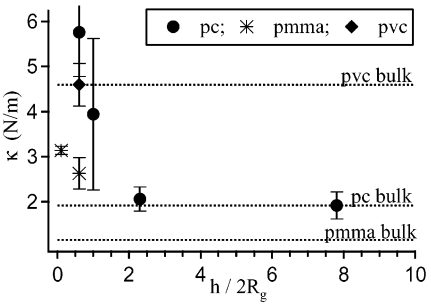

Figure 5. Variations in the vibrational spring constant κ are displayed as a function of the normalized film thickness, with the dashed lines indicating κ for the bulk material. PC exhibits strong vibrational stiffening with decreasing film thickness while PVC remains bulklike even in the R_g-thick film. The vertical errors indicate the standard uncertainties of κ.

both the Stokes−Einstein (diffusion and viscosity) and Debye-Einstein (reorientation time and viscosity) relationships,[47−49] a bifurcation of the α- and β-relaxation processes,[47,50,51] the breaking of ergodicity as predicted by mode coupling theory,[52,53] and a crossover between the two Vogel−Fulcher relations commonly needed to fit relaxation data above T_g.[54−59] Thus, there is a strong precedent for a characteristic glass formation temperature near $(1.2-1.5)T_g$. That this characteristic temperature is on the order of $1.2T_g$ is also consistent with the fact that polymers generally lie on the fragile end of this glass-forming classification scheme. However, this does not explain why such an upper transition temperature would be exacerbated in the exceedingly thin films. At this point we can only speculate why the $1.2T_g$ characteristic temperature is emphasized in the thin films.

Vibrational Stiffening in Thin Polymer Films. As discussed above, the estimate of $\langle u^2 \rangle$ from eq 1 is based on a harmonic approximation, which is strictly violated by the high-temperature, nonlinear regimes in Figures 3 and 4. However, below 200 K the thermal evolution of $\langle u^2 \rangle$ is linear, and it is reasonable to assume that the atoms are trapped in local minima of the potential energy landscape. In this regime, the equipartition theorem allow us to quantify the stiffness or resistance to displacement in terms of a harmonic force constant κ, where $\kappa = 3k_BT/\langle u^2 \rangle$. The low-temperature slope of $\langle u^2 \rangle$ vs T is inversely proportional to the elastic force constant κ. In this picture, the confinement-induced suppression of $\langle u^2 \rangle$ indicates an increase in the vibrational stiffness. Figure 5 summarizes these variations of κ as a function of film thickness h (normalized by $2R_g$, nominally the diameter of the macromolecule) for the three polymers. For comparison, the dashed lines indicate the κ for the bulk materials. Broadly speaking, κ ranges from 1 to 6 N/m in the polymer thin films. These values are reasonable in that they are comparable with analogous measurements on proteins below 200 K.[11] Likewise, the κ for pure Si is reported to be 78.5 N/m,[69] 1−2 orders of magnitude greater than the polymer reported here. This is consistent with the fact that elastic modulus of Si is also 1−2 orders of magnitude greater than most polymers.

Figure 5 indicates that thin film confinement significantly stiffens the local motions of PC, while virtually no changes are observed in PVC. This is consistent with the earlier discussion of the extensive molecular mobility in glassy PC. Confinement curtails the longer-range glassy motions as indicated by the elastic stiffening, whereby the predominantly localized motions of PVC are unchanged. Of course, one must be cognizant of the nature of these motions. We already discussed how phenyl ring and methyl group motions in the PC are emphasized in $\langle u^2 \rangle$. To this end, when these motions are constrained in the 75 Å PC film ($\kappa = 5.8 \pm 1.0$ N/m), it is notable, and somewhat reassuring, that that elastic stiffness is then equivalent to bulk PVC ($\kappa = 4.6 \pm 0.5$ N/m) where these motions are naturally absent and κ more truly reflects interchain vibrations. As with the amplitudes of $\langle u^2 \rangle$, PC and PVC represent the extremes in terms of the low-temperature vibrational stiffening. The R_g-thick PC, PMMA, and PVC films stiffen by approximately 200%, 130%, and 0%, respectively, in comparison to the bulk vibrations. In short, thin film confinement increases the degree of intermolecular caging in those glasses that naturally possess extensive mobility. This caging effect is evident over a wide range of length scales, extending from the low-temperature harmonic vibrations to the long-range diffusive motion that occur above the glass transition temperature. There can be a considerable reduction of a polymer's mobility as it is confined to a thin polymer film.

Given the wide range of data that we have presented here, it appears that the reduction of mobility or $\langle u^2 \rangle$ is a geometric aspect of confinement, independent of the interactions with the confining surface. This is supported by the fact that $\langle u^2 \rangle$ is equally suppressed in thin PMMA films supported on both the native oxide (favorable) and HMDS (unfavorable) substrates. While this may seem to contradict the optical[40,41] and thermal probe[42] measurements, we liken our findings to surface forces measurements of the shear viscosity in exceedingly thin liquid films. These measurements show that the geometric aspect of confinement induces efficient intermolecular packing when the film thickness approaches nominally 10 times the molecular diameter (approximately 100−200 Å in most polymers). This leads to an *increase* in the shear viscosity and the elastic properties of the film, regardless of the interactions between the confining mica rods of the surface forces apparatus and the liquid.[43−46] These observations are phenomenologically relevant given the notable correlation between $\langle u^2 \rangle$ and viscosity;[61,62] the viscosity appears to increases exponentially with $1/\langle u^2 \rangle$. In this respect the reduction of $\langle u^2 \rangle$ with decreasing film thickness is consistent with an increase of viscosity.

Taken together, the neutron scattering and surface forces measurements appear to suggest that mobility or the amplitude of the thermal motion is always reduced in thin, supported polymer film. If true, this is an extremely important distinction. From an applications point of view, a large number of the studies focus on identifying an apparent kink or T_g shift as evidence for thin film property deviations. From the discussion above, this could potentially lead to an erroneous interpretation. For example, we motivated this discussion through the example of photoacid diffusion in a thin resist film. If the hypothetical resist were the thin PC film, the apparent T_g decrease from X-ray reflectivity and PALS might lead to the conclusion that the kinetics of photoacid transport would be enhanced at temperatures near the bulk glass transition. However, if the overall mobility is reduced, the relative T_g kink may be *irrelevant*, and ultimately the kinetics could be hindered with respect to very thick films. Clearly, great care must still be exercised in interpreting T_g shift data from thin polymer films.

Conclusions

Incoherent neutron scattering measurements are performed on a series polycarbonate (PC), poly(methyl methacrylate) (PMMA), and poly(vinyl chloride) (PVC) films as thin as 75 Å supported on a silicon wafer. As the temperature increases, there is a decrease in the intensity of the elastically scattered neutrons, and this increase in polymer's vibrational density of states is approximated through the mean-square atomic displacement $\langle u^2 \rangle$ within the harmonic Debye−Waller formalism. Above the calorimetric T_g of the bulk polymer there is a ubiquitous decrease of $\langle u^2 \rangle$ as the film thickness decreases. However, below T_g the magnitude of the reduction is proportional to the $\langle u^2 \rangle$ in the native glass. PC has a very large $\langle u^2 \rangle$ in the bulk glass, and correspondingly a strong reduction in the thin film, while PVC has a small $\langle u^2 \rangle$ in the bulk glass and no reduction in the thin film. In the glass, we demonstrate that molecular motions reflected in larger $\langle u^2 \rangle$ values are localized segmental motions of the hydrogen moieties, i.e., methyl and/or phenyl group librations/rotations. It is generally understood that $\langle u^2 \rangle$ experiences a strong upturn near the calorimetric T_g, reflecting the sudden onset of fluidity. The thin film measurements indicate that this upturn is shifted to higher temperatures as the film thickness is reduced which would seemingly indicate an increase of the thin film T_g. However, there are discrepancies between $\langle u^2 \rangle$ and the other techniques commonly used to characterize the glass transition in thin polymer films that point to a T_g decrease. While the explanation for these discrepancies remains unclear, possibilities are discussed in terms of the characteristic frequencies of the various techniques. Regardless of the nature of the glass transition in thin polymer films, at low temperatures, well below T_g, there is a strong reduction of $\langle u^2 \rangle$ upon confinement in the highly dynamic (larger $\langle u^2 \rangle$) glassy polymer, and this is quantified in terms of stiffening of the harmonic vibrations or an increased intermolecular caging.

Acknowledgment. The authors are grateful to Dan Neumann for his critical review of the manuscript and many insightful discussions. This work is based upon activities supported by the National Science Foundation under Agreement DMR-0086210.

References and Notes

(1) Forrest, J. A.; Dalnoki-Verres, K. *Adv. Colloid Interface Sci.* **2001**, *94*, 167.
(2) Frick, B. *Prog. Colloid Polym. Sci.* **1989**, *80*, 164.
(3) Frick, B.; Fetters, L. J. *Macromolecules* **1997**, *27*, 9974.
(4) Frick, B.; Richter, D. *Science* **1995**, *267*, 1939.
(5) Colmenero, J.; Arbe, A. *Phys. Rev. B* **1998**, *57*, 13508.
(6) Angell, C. A.; Ngai, K. L.; McKenna, G. B.; McMillan, P. F.; Martin, S. W. *J. Appl. Phys.* **2000**, *88*, 3113.
(7) Doster, W.; Cusack, S.; Petry, W. *Nature (London)* **1989**, *337*, 754.
(8) Angell, C. A. *Science* **1995**, *267*, 1924.
(9) Lehnert, U.; Réat, Weik, M.; Zaccaï, G.; Pfiester, C. *Biophys. J.* **1998**, *75*, 1945.
(10) Deriu, A. *Neutron News* **2000**, *11*, 26.
(11) Zaccaï, G. *Science* **2000**, *288*, 1604.
(12) Soles, C. L.; Douglas, J. F.; Wu, W.-l.; Dimeo, R. M. *Phys. Rev. Lett.* **2002**, *88*, 7401.
(13) Certain commercial equipment and materials are identified in this paper in order to specify adequately the experimental procedure. In no case does such identification imply recommendation by the National Institute of Standards and Technology nor does it imply that the material or equipment identified is necessarily the best available for this purpose.
(14) Gehring, P. M.; Neumann, D. A. *Physica B* **1998**, *241−243*, 64.
(15) Settles, M.; Doster, W. *Faraday Discuss.* **1996**, *103*, 269.
(16) Prevorsek, D. C.; DeBona, B. T. *J. Macromol. Sci., Phys.* **1986**, *B25*, 515.
(17) Chinai, S. N.; Guzzi, R. A. *J. Polym. Sci.* **1959**, *41*, 475.
(18) Sato, M.; Koshiishi, Y.; Asahina, M. *Polym. Lett.* **1963**, *1*, 233.
(19) Garfield, L. J. *J. Polym. Sci., Part C* **1970**, *30*, 551.
(20) Spiess, H. W. *Colloid Polym. Sci.* **1983**, *261*, 193.
(21) Schaefer, J.; Stejskal, E. O.; McKay, R. A.; Dixon, W. T. *Macromolecules* **1984**, *17*, 1479.
(22) Schmidt, C.; Kuhn, K. J.; Spiess, H. W. *Prog. Colloid Polym. Sci.* **1985**, *71*, 71.
(23) Smith, P. B.; Brubeck, R. A.; Bales, S. E. *Macromolecules* **1988**, *21*, 2058.
(24) Steger, T. R.; Schaefer, J.; Stejskal, E. O.; Mckay, R. A. *Macromolecules* **1980**, *13*, 1127.
(25) Jones, A. A.; O'Gara, J. F.; Inglefield, P. T.; Bendler, J. T.; Yee, A. F.; Ngai, K. L. *Macromolecules* **1983**, *16*, 658.
(26) Roy, A. K.; Jones, A. A.; Inglefield, P. T. *Macromolecules* **1986**, *19*, 1356.
(27) Wehrle, M.; Hellmann, G. P.; Spiess, H. W. *Colloid Polym. Sci.* **1987**, *265*, 815.
(28) Reading, F. P.; Faucher, J. A.; Whitman, R. D. *J. Polym. Sci.* **1961**, *54*, 556.
(29) Matsuoka, S.; Ishida, Y. *J. Polym. Sci., Part C* **1966**, *14*, 247.
(30) Stefan, D.; Williams, H. L. *J. Appl. Polym. Sci.* **1974**, *18*, 1279.
(31) Watts, D. C.; Perry, E. P. *Polymer* **1978**, *19*, 248.
(32) McCrum, N. G.; Read, B. E.; Williams, G. *Anelastic and Dielectric Effects in Polymeric Solids*; John Wiley and Sons: London, 1967.
(33) Liu, J.; Yee, A. F. *Macromolecules* **1998**, *31*, 7865.
(34) Wu, J.; Xiao, C.; Klug, C. A.; Schaefer, J. *J. Polym. Sci., Part B: Polym. Phys.* **2001**, *39*, 1730.
(35) Davenport, W. A.; Manuel, A. J. *Polymer* **1977**, *18*, 557.
(36) Schaefer, J.; Stejskal, F. O.; Buchdahl, R. *Macromolecules* **1977**, *10*, 384.
(37) Frick, B.; Richter, D.; Petry, W.; Buchenau, U. *Z. Phys. B: Condens. Matter* **1988**, *70*, 73.
(38) Ngai, K. L.; Bao, L.-R.; Yee, A. F.; Soles, C. L. *Phys. Rev. Lett.* **2001**, *87*, 5901.
(39) Soles, C. L.; Douglas, J. F.; Wu, W.-l.; Peng, H.; Gidley, D. W. *MRS Proc.*, in press.
(40) Keddie, J. L.; Jones, R. A. L.; Cory, R. A. *Faraday Dicsuss.* **1994**, *98*, 1.
(41) Prucker, O.; Christian, S.; Bock, H.; Ruhe, J.; Frank, C. W.; Knoll, W. *Macromol. Chem. Phys.* **1998**, *199*, 1435.
(42) Fryer, D. S.; Nealy, P. F.; de Pablo, J. J. *Macromolecules* **2000**, *33*, 6439.
(43) Horn, R. G.; Israelachvili, J. N. *Macromolecules* **1988**, *21*, 2836.
(44) Granick, S. *Science* **1991**, *253*, 1374.
(45) Hu, H.-W.; Granick, S. *Science* **1992**, *258*, 1339.
(46) Levent Demirel, A.; Granick, S. *Phys. Rev. Lett.* **1996**, *77*, 2261.
(47) Rossler, E. *Phys. Rev. Lett.* **1990**, *65*, 1595.
(48) Fujara, F.; Geil, B.; Sillescu, H.; Fleischer, G. *Z. Phys. B* **1992**, *88*, 195.
(49) Chang, I.; Fujara, F.; Heuberger, B. G. G.; Mangel, T.; Sillescu, H. *J. Non-Cryst. Solids* **1994**, *172−174*, 248.
(50) Hansen, C.; Stickel, F.; Berger, T.; Richert, R.; Fischer, E. W. *J. Chem. Phys.* **1997**, *107*, 1086.
(51) Hansen, C.; Stickel, F.; Richert, R.; Fischer, E. W. *J. Chem. Phys.* **1998**, *108*, 6408.
(52) Gotze, W.; Sjogren, L. *Rep. Prog. Phys.* **1992**, *55*, 241.
(53) Gotze, W. *J. Phys.: Condens. Matter* **1991**, *11*, A1.
(54) Plazek, D. J.; Magill, J. H. *J. Chem. Phys.* **1966**, *45*, 3038.
(55) Greet, R. J.; Magill, J. H. *J. Phys. Chem.* **1967**, *71*, 1746.
(56) Plazek, D. J.; Magill, J. H. *J. Chem. Phys.* **1968**, *49*, 3678.
(57) Stickel, F.; Fischer, E. W.; Richert, R. *J. Chem. Phys.* **1995**, *102*, 6251.
(58) Stickel, F.; Fischer, E. W.; Richert, R. *J. Chem. Phys.* **1996**, *104*, 2043.
(59) Ngai, K. L.; Magill, J.; Plazek, D. *J. Chem. Phys.* **2000**, *112*, 1887.
(60) Flensburg, C.; Stewart, R. F. *Phys. Rev. B* **1999**, *60*, 284.
(61) Bucheneau, U.; Zorn, R. *Europhys. Lett.* **1992**, *18*, 523.
(62) Kanaya, T.; Tsukushi, T.; Kaji, K.; Bartos, J.; Kristiak, J. *Phys. Rev. E* **1992**, *60*, 1906.

MA020952K